Wiley Online Library
Early View publication on www.wileyonlinelibrary.com
(issue and page numbers not yet assigned;
citable using Digital Object Identifier – **DOI**)

Phys. Status Solidi A, 1700018 (2017) / **DOI** 10.1002/pssa.201700018

physica status solidi a
www.pss-a.com
applications and materials science

Characteristics of PTB7-Th:C_{70} bulk heterojunction photocells under low-light illumination: Critical effect of dark parallel resistance

Kazuya Tada*

Division of Electrical Materials and Engineering, University of Hyogo, 2167 Shosha, Himeji, Hyogo 671-2280, Japan

Received 11 January 2017, revised 28 February 2017, accepted 20 March 2017
Published online 12 April 2017

Keywords conjugated polymers, fullerenes, halogen-free solvents, light harvesting, organic photovoltaics

* e-mail tada@eng.u-hyogo.ac.jp, Phone: + 81-79-267-4966, Fax: +81-79-267-4855

Solution-processed organic photocell is one of the most promising candidates for the permanent power source for wireless devices. Since the device is not necessarily to be placed outdoor, and indoor light is generally weaker than outdoor light by 2–3 orders of magnitude, the characterization of the photocell under low-light illumination is important for this purpose. In this study, bulk heterojunction photocells based on a low-energy gap polymer poly[[4,8-bis[5-(2-ethylhexyl)thiophene-2-yl]benzo[1,2-b:4,5-b′]dithiophene-2,6-diyl][3-fluoro-2-[(2-ethylhexyl)carbonyl]thieno[3,4-b]thiophenediyl]] (PTB7-Th) as well as unmodified C_{70} prepared with a halogen-free solvent 1,2,4-trimethylbenzene, are characterized under low-light illumination. The combination of a halogen-free solvent with an unmodified fullerene potentially provides a way to develop environmentally friendly organic photocells. It is found that the photocells show higher power conversion efficiency (PCE) under lower light illumination intensity. That is, a device showing PCE of 4.9% under 1 sun illumination shows PCE over 9% at 3' 10^{-4} sun. A sublinear dependence of the short-circuit photocurrent to the light intensity, as well as the increased fill-factor at reduced illumination, is found to be a key to the high PCE at low-light. The latter originates from the photoconduction in the composite. The critical effect of dark parallel resistance on the low-light performance of the photocells is also demonstrated.

1 Introduction Photocells based on bulk heterojunction composites consisting of conjugated polymers and fullerenes are attracting much interest of the researchers, partly because the compatibility with low-temperature solution-based process makes them promising candidates for large-area low-cost renewable energy source in the near future [1–4]. The development of conjugated polymers such as poly[[4,8-bis[(2-ethylhexyl)oxy]benzo[1,2-b:4,5-b′]dithiophene-2,6-diyl][3-fluoro-2-[(2-ethylhexyl)carbonyl]thieno[3,4-b]thiophenediyl]] (PTB7) and poly[[4,8-bis[5-(2-ethylhexyl) thiophene-2-yl]benzo[1,2-b:4,5-b'f]dithiophene-2,6-diyl][3-fluoro-2-[(2-ethylhexyl)carbonyl]thieno [3,4-b]thiophenediyl]] (PTB7-Th) is pushing up the performance of this class of photocells [5, 6].

The use of highly soluble fullerene derivatives such as [6,6]-phenyl-C_{71}-butyric acid methyl ester (C_{70}-PCBM), as well as the use of chloroaromatic solvents, is known as the best practice in the field of solution-processed polymer photocells study at present. However, a life-cycle assessment study of the solution-processed photocells has pointed out that replacement of fullerene derivatives with unmodified fullerene effectively reduces the environmental and economical cost of the device [7]. In addition, the use of halogenated compounds including chloroaromatic solvents is not generally preferred in industrial production, because such compounds have biological and environmental toxicity [8, 9]. Thus, the realization of solution-processed polymer photocells with unmodified fullerene by using a halogen-free solvent seems to be an attractive research subject. The author has shown that a not-so-common halogen-free solvent 1,2,4-trimethylbenzene (TMB), also known as pseudocumene, enables the production of polymer bulk heterojunction composites with unmodified fullerene such as C_{60} and C_{70} for

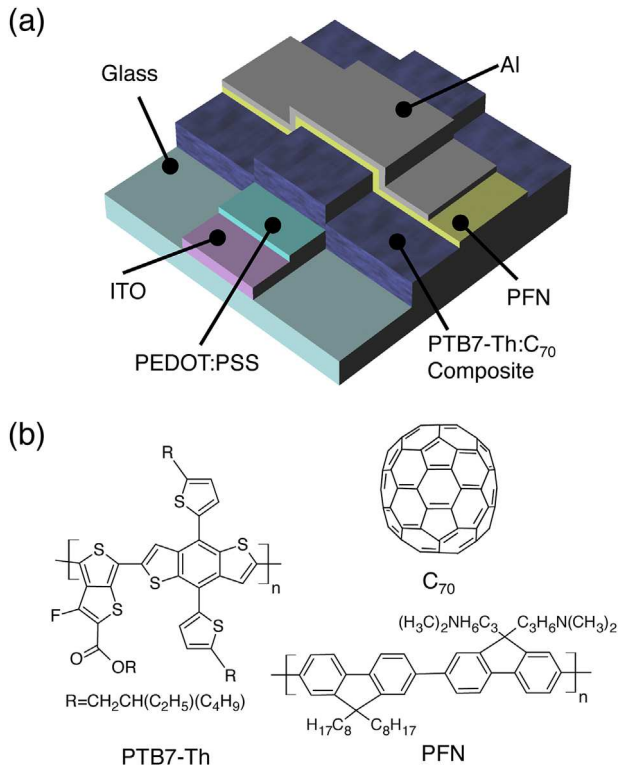

Figure 1 (a) Schematic structure of the photocell and (b) molecular structures of key materials used in this study.

photocells [10–13]. Recently, TMB has attracted special attention of researchers as a promising green solvent for polymer photocells [14, 15].

Although the development of outdoor large-area photocells, which will be connected to electric power grid, is quite important, photocells are also useful as a standalone power source for indoor equipments. Wireless sensor networks, urgently spreading in modern society and suitable electric power sources, which harvest small ambient energy for the sensor nodes, have been extensively studied. The indoor light intensity is generally expected to be smaller than the outdoor one by 2–3 orders of magnitude [16–18]. For this purpose, the characterization, as well as the development of suitable circuit model of a photocell under low-light illumination, is essential. Recent studies have shown that polymer photocells are promising for indoor light harvesting [19–22].

In this study, the characteristics of photocells with PTB7-Th:C_{70} bulk heterojunction composite, which show the power

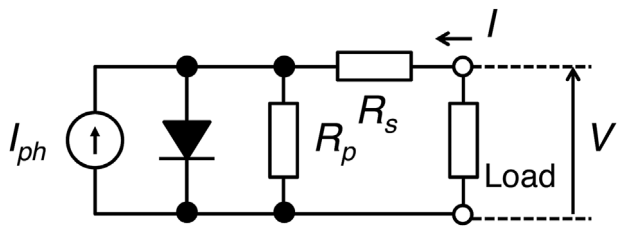

Figure 2 1-diode equivalent circuit model.

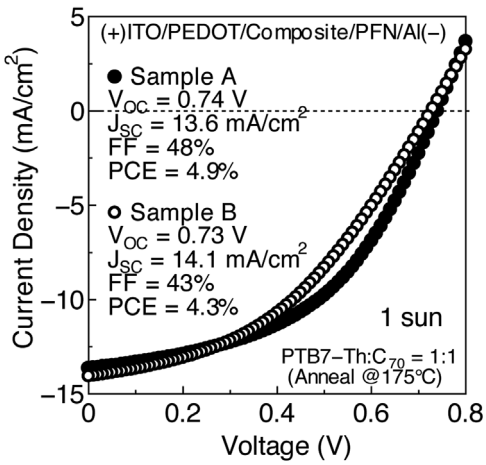

Figure 3 Current density–voltage characteristics of the PTB7-Th:C_{70} photocells under 1 sun illumination.

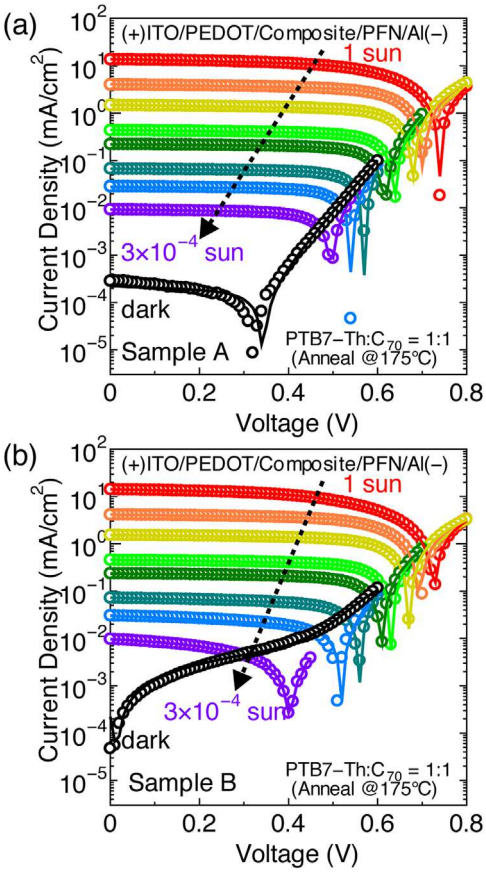

Figure 4 Semilogarithmic plots of current density–voltage characteristics of the PTB7-Th:C_{70} photocells at various illumination intensities. (a) and (b), respectively, correspond to the samples A and B. Experimental data and fitting curves are indicated as symbols and lines, respectively.

conversion efficiency (PCE) close to 5% at AM 1.5G 1 sun illumination [13] under low-light illumination, are studied. A sublinear dependence of the short-circuit photocurrent on the illumination light intensity, as well as increased fill-factor

(FF) under reduced illumination, is identified as the key to the improvement of PCE under low light. The analysis using one-diode equivalent circuit model revealed that the higher FF at lower illumination light intensity originates from the reciprocal proportionality of the parallel resistance to the illumination light intensity, as well as the decreased reverse saturation current of the diode, under reduced illumination. On the other hand, the deep highest occupied molecular orbital (HOMO) level of PTB7-Th yields higher PCE at reduced illumination in the PTB7-Th:C_{70} photocell than that in the PTB7:C_{70} photocell. In addition, the importance of the dark parallel resistance of a photocell for its low-light characteristics is mentioned.

2 Experimental Photocells with ITO/PEDOT:PSS/PTB7-Th:C_{70}/PFN/Al structure are used in this study. Figure 1 shows the schematic device structure of photocells, as well as the molecular structures of the key materials. In this structure, PEDOT:PSS and PFN stand for poly(3,4-dioxythiophene):poly(styrene sulfonate) salt and poly[9,9-bis(3′-(N,N-dimethyl)-propyl-2,7-fluorene)-*alt*-2,7-(9,9-dioctylfluorene)], which function as hole- and electron-transporting layers, respectively. PTB7-Th (also known as PCE10) and PFN were purchased from 1-Material. C_{70} was the product of Nano-C. All chemicals including TMB from Tokyo Kasei were used as received.

The photocells were fabricated as follows. A film of PEDOT:PSS was deposited on a glass substrate with a pre-patterned ITO electrode by spin-coating from an aqueous suspension purchased from Aldrich, followed by annealing at 130 °C for 60 min in air. The thickness of the PEDOT:PSS film was approximately 50 nm. Then, the substrate was transferred to a glove-box filled with nitrogen. A 60 nm-thick film of PTB7-Th:C_{70} composite (1:1 by weight) was coated on the PEDOT:PSS film at a spin-rate of 1500 rpm for 30 s from a composite solution dissolved in TMB. The total concentration of the composite solution was 30 g l^{-1}. Since the PTB7-Th sample used for the present study was less soluble in TMB than that used in the previous study [13], the composite solution had to be warmed upon a hotplate at 100 °C for a few hours prior to the spin-coating. A 1.0 g l^{-1} stock solution of PFN dissolved in methanol containing 2 vol.% of acetic acid was diluted with pure methanol to obtain 0.3 g l^{-1} PFN solution. The spin-coating of a PFN layer on the composite film was carried out at a spin-rate of 3000 rpm for 5 s from the 0.3 g l^{-1} PFN solution. The PFN film was so thin that its thickness is unknown. After the vacuum deposition of an Al cathode on the PFN layer, the device was subjected to thermal annealing on a hotplate heated at 175 °C for 20 min. The active area of the photocells is 3 mm × 3 mm. The active area of the photocell was covered by a glass plate and a UV-curable resin to avoid prompt degradation in air.

The current–voltage characteristics are measured with a Keithley 2400 source-meter in air. The light source used was an Asahi Spectra HAL-C100 solar simulator with AM1.5G 1 sun (100 mW cm^{-2}) illumination and the light intensity was

Table 1 Circuit parameters of the PTB7-Th:C_{70} photocells under dark and 1 sun illumination obtained by curve-fitting. *A* denotes the active area of the photocells.

	sample A		sample B	
	dark	1 sun	dark	1 sun
J_{ph} [mA/cm]	2.2×10^{-4}	15.3	2.2×10^{-4}	16.6
J_S [nA/cm]	2.8×10^{-2}	8.1×10^{-2}	6.1×10^{-2}	1.2×10^{-1}
$R_S \cdot A$ [Ω · cm^2]	13	15	33	21
$R_p \cdot A$ [Ω · cm^2]	5.7×10^6	1.5×10^2	6.5×10^4	1.3×10^2
n	1.52			

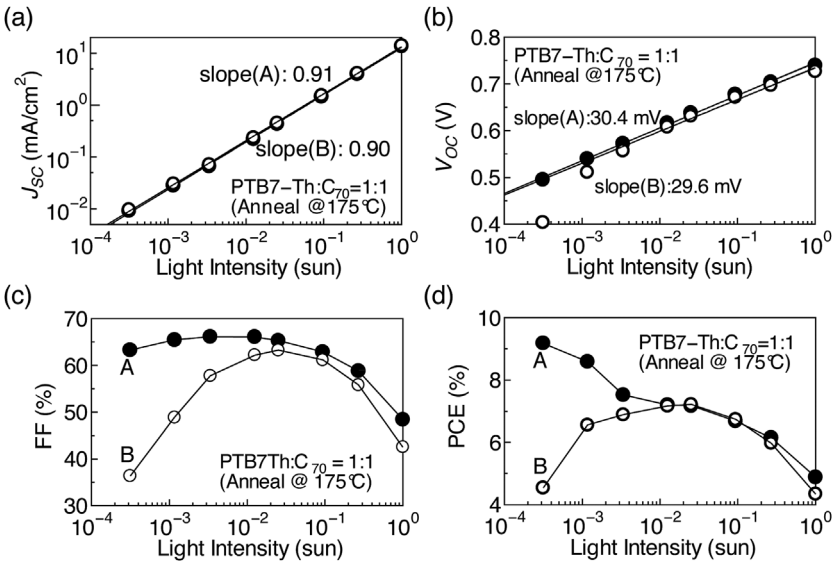

Figure 5 Illumination light intensity dependences of (a)J_{SC}, (b) V_{OC}, (c) FF, and (d) PCE of the PTB7-Th:C_{70} photocells. Closed and open symbols correspond to the samples A and B, respectively.

reduced by a set of neutral density (ND) filters. The reduction factors of the illumination light intensity were calculated from the optical transmission spectra of the ND filters as well as the AM 1.5G 1 sun spectra in the range of 350–750 nm. The fitting of current–voltage characteristics with the one-diode equivalent circuit model shown in Fig. 2, whose current–voltage characteristic is expressed as

$$I = I_s \cdot \left(\exp\left(\frac{V - I \cdot R_s}{n \cdot V_t} \right) - 1 \right) + \frac{V - I \cdot R_s}{R_p} - I_{ph} \quad (1)$$

was carried out by using the Solver function of Microsoft Excel 2007 in order to extract the circuit parameters of the device [23]. In this equation, the I_{ph} denotes the ideal photocurrent source, while the saturation current I_s and the ideality factor n are the parameters of the diode. The R_s and R_p stand for the series resistance and parallel (shunt) resistance, respectively. The thermal voltage V_t is 26 mV at room temperature.

The morphology of a PTB7-Th:C_{70} composite film coated on a glass plate was observed by using a NanoMagnetics ezAFM atomic-force microscope (AFM) in tapping-mode. The AFM images were processed with WSXM software [24, 25].

3 Results and discussion Here, the characteristics of two PTB7-Th:C_{70} photocell samples (A and B), whose current density–voltage curves under 1 sun shown in Fig. 3, are discussed. The PCE at 1 sun of sample A is 4.9% and is slightly higher than that of sample B, 4.3%. However, the difference is within the error range and is not significant. In other words, both of them are apparently healthy devices. Figure 4 shows the current density–voltage characteristics of the PTB7-Th:C_{70} photocells under various illumination light intensities. For both of the samples, the short-circuit current density (J_{SC}) as well as the open-circuit voltage (V_{OC}) monotonically decrease as the illumination weakens.

It is noticed that sample A showed a small short-circuit current under dark. Although the precise reason for this is not clear at this stage, some electrochemical effects within the device probably yield the dark current. Since the dark short-circuit current is 40 times smaller than the short-circuit current under the lowest illumination light intensity tested 3×10^{-4} sun, we can ignore its effect on the characteristics under the illuminations tested. The fitting of the dark characteristics with the equivalent circuit model yields the n of 1.52, and this value is used in the curve fittings throughout the present study. On the other hand, the dark characteristics of the sample B shows negligible short-circuit current. Table 2 summarizes the circuit parameters of the photocells under dark and 1 sun illumination, extracted by the curve-fitting. The parameters presented are normalized to the device area A. All of the parameters listed, except for the R_p, under dark seem to be independent of the samples. The dark R_p of sample B is found to be smaller than that of the sample A by two orders of magnitude. This makes the dark short-circuit current in the fitting curve of sample B negligible, as shown in Fig. 4b, even if the same J_{ph} under dark as sample A is expected.

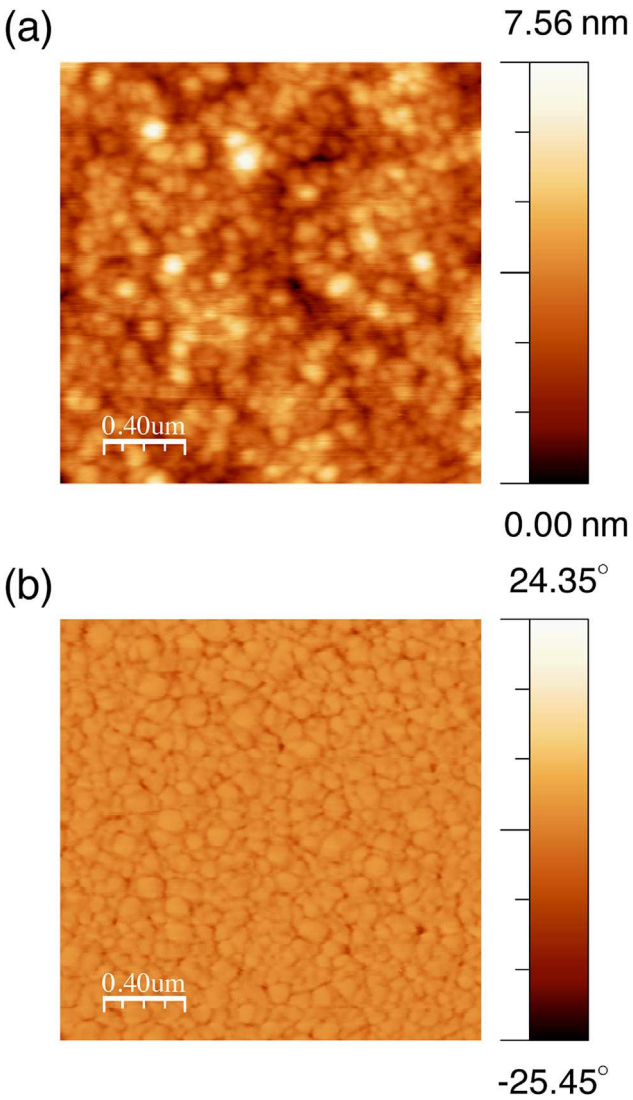

Figure 6 (a) Height and (b) phase images of the PTB7-Th:C_{70} composite film taken by AFM. Scanned area: 2 μm × 2 μm.

The dependences of J_{SC}, V_{OC}, FF, and PCE of the photocells on the illumination light intensity are presented in Fig. 5. The dependences of J_{SC} are expressed by a power function with a single exponent close to 0.9 for both samples. The sublinear dependence on the light intensity is key to high PCE at low illumination light intensity, since this gives higher photocurrent per unit photon flux at lower illumination light intensity. It has been pointed out that this characteristic can be explained by exponentially distributed traps near the band edges [26]. On the other hand, the slope found in the semilogarithmic plot of the V_{OC} versus the illumination light intensity is approximately 30 mV for both samples. The slope exceeding the thermal voltage 26 mV, which corresponds to the trap-free case where the bimolecular

recombination solely takes place, suggests the contribution of trap-assisted recombination process under the open-circuit condition [27]. It can be noticed that the V_{OC} of sample B deviates from the straight line when the illumination is lower than 10^{-2} sun.

To obtain deeper insight into the origin of the traps, the morphology of the composite film is observed by AFM. The height image shown in Fig. 6a, as well as the phase image shown in Fig. 6b, depict the domains with a few hundred nanometer size, being consistent with the reported value for PTB7:C_{70}-PCBM composite without additives, such as 1,8-diiodooctane [28, 29]. Since the domain size observed is much larger than typical diffusion length of the excitons in organic semiconductors [30], the size of the domain seems to be a major source of the traps.

The FF of the device increases with decreasing illumination light intensity, being also key to high PCE at low illumination light intensity. In summary, the PCE increases with decreasing illumination light intensity. That is, sample A, whose PCE under 1 sun illumination is 4.9%, shows a PCE of 9.2% at 3×10^{-4} sun. In comparison with the previously reported PTB7-based device [22], the PCE under 1 sun, as well as that under 3×10^{-4} sun, in the present PTB7-Th-based photocell is high. This comes from the deeper HOMO level of PTB7-Th than that of PTB7 by 0.07 eV, resulting in the improvement of the V_{OC} from the PTB7-based photocell (0.70 V at 1 sun) to the present PTB7-Th-based photocell (0.74 V at 1 sun) [31]. The lowest unoccupied molecular orbital (LUMO) level of a unmodified fullerene is generally deeper than that of the PCBM-type counterpart by 0.1–0.2 eV [32], suggesting that unmodified fullerenes potentially offer high performance bulk heterojunction photocells using some polymers, whose LUMO level is so low that it is not compatible with the PCBM-type fullerenes. Although the FF of sample A monotonically increases with decreasing illumination light intensity down to 3×10^{-3} sun and then saturates, the FF of sample B quickly drops for illumination light intensity lower than 3×10^{-2} sun, resulting in the quick drop of the PCE. The PCE of sample B at 3×10^{-4} sun is approximately 4.5%.

Figure 7 summarizes the dependence of the circuit parameters of the photocells extracted by the curve-fitting on the illumination light intensity. The parameters presented are normalized to the device area A. The dependence of the ideal photocurrent density J_{ph} is almost identical to that of J_{SC}. The most significant change is observed in R_p, which is almost inversely proportional to the illumination light intensity. Together with the positive correlation of J_s to illumination light intensity, this is probably key to the increased FF at low illumination light intensity, since both of them correspond to the reduction of the photocarrier loss in the device at reduced illumination light intensity. Both of them seem to come from the increased carrier density in bulk heterojunction composite upon illumination, or photoconductive effect [33]. This may also account for the increase of R_s at decreased illumination light intensity.

The most significant difference between the samples is also observed in R_p. That is, the R_p of sample B tends to saturate when the illumination light intensity is lower than 10^{-2} sun. This results in the drops found in V_{OC} and FF at low light because other parameters are almost independent of the sample. The saturation comes from the low dark R_p of the sample, since the R_p under illumination can be expressed as the parallel connection of the dark R_p and the purely photoconductive part which is reciprocal to the illumination light intensity and becomes infinity under dark. Indeed, the resistance calculated in that manner reasonably reproduces the

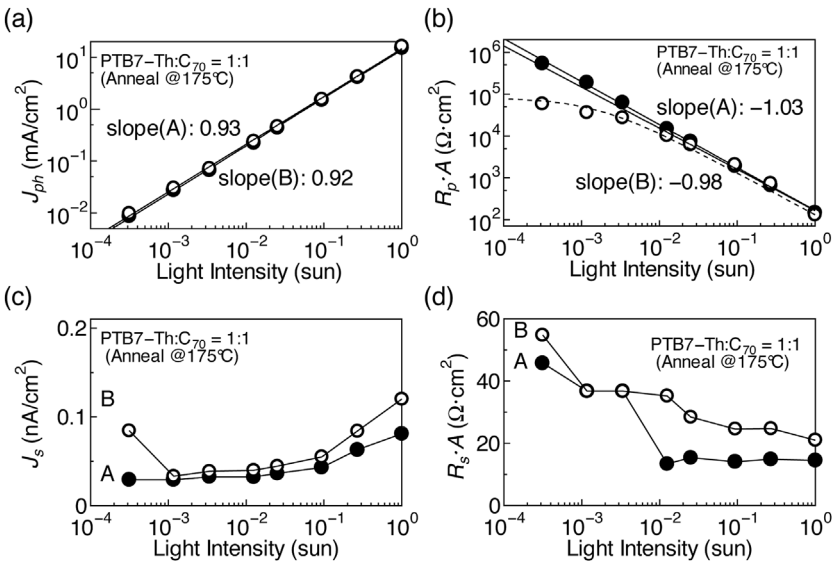

Figure 7 Illumination light intensity dependences of (a)J_{ph}, (b)$R_p \cdot A$, (c) J_s, and (d) $R_s \cdot A$ of the PTB7-Th:C_{70} photocells, where A denotes the active area of the photocell. Closed and open symbols correspond to samples A and B, respectively. Dashed line in (b) shows the calculated resistance for the sample B.

R_p observed as shown in Fig. 7b. Some defect in the device, such as pin-hole probably, lowers the dark R_p of a photocell. However, it cannot be detected by the characterization under 1 sun, since the total conductance is dominated by the photoconductive part.

4 Conclusions In this study, the low-light characterization of PTB7-Th:C_{70} bulk heterojunction photocells prepared with halogen-free TMB are carried out. The device showing PCE of 4.9% under 1 sun illumination shows PCE over 9% at 3×10^{-4} sun. It has been shown that the sublinear dependence of the short-circuit photocurrent to the light intensity, as well as the increase of FF under low illumination light intensity, is key to the high PCE at low illumination light intensity. The hundred-nanometer-sized domains observed by AFM seem to be the source of the traps, which give the sublinear dependence of the short-circuit photocurrent to the light intensity. The impact of dark parallel resistance on the low-light performance of a photocell is experimentally demonstrated. The results mentioned in the present study suggest that the polymer bulk heterojunction photocells with unmodified fullerene prepared from halogen-free solvent are potentially useful for environmentally friendly indoor light harvesting devices.

Acknowledgement This work was partially supported by JSPS KAKENHI Grant Number JP26289094.

References

[1] A. J. Heeger, Adv. Mater. **26**, 10 (2014).
[2] G. Li, R. Zhu, and Y. Yang, Nature Photon. **6**, 153 (2012).
[3] H. Jin, A. Armin, M. Hambsch, Q. Lin, P. L. Burn, and P. Meredith, Phys. Status Solidi A **212**, 224 (2015).
[4] T. Hahn, C. Saller, M. Weigl, I. Bauer, T. Unger, A. Kohler, and P. Strohriegl, Phys. Status Solidi A **212**, 2162 (2015).
[5] Z. He, C. Zhong, X. Huang, W.-Y. Wong, H. Wu, L. Chen, S. Su, and Y. Cao, Adv. Mater. **23**, 4634 (2012).
[6] S.-H. Liao, H.-J. Jhuo, Y.-S. Cheng, and S.-A. Chen, Adv. Mater. **25**, 4766 (2013).
[7] A. Anctil, C. W. Babbitt, R. P. Raffaelle, and B. J. Landi, Prog. Photovolt. **21**, 1541 (2013).
[8] P. Tundo, Pure Appl. Chem. **84**, 411 (2012).
[9] B. Schmidt-Hansberg, M. Sanyal, N. Grossiord, Y. Galagan, M. Baunach, M. F. G. Klein, A. Colsmann, P. Scharfer, U. LemmerDosch, H. Dosch, J. Michels, E. Barrena, and W. Schabel, Sol. Energy Mater. Sol. Cells **96**, 195 (2012).
[10] K. Tada, Sol. Energy Mater. Sol. Cells **108**, 82 (2013).
[11] K. Tada, Sol. Energy Mater. Sol. Cells **112**, 194 (2013).
[12] K. Tada, Sol. Energy Mater. Sol. Cells **132**, 15 (2015).
[13] K. Tada, Sol. Energy Mater. Sol. Cells **143**, 52 (2015).
[14] C. -C. Chueh, K. Yao, H. -L. Yip, C. -Y. Chang, Y. -X. Xu, K. -S. Chen, C. -Z. Li, P. Liu, F. Huang, Y. Chen, W. -C. Chen, and A. K. -Y. Jen, Energy Environ. Sci. **6**, 3241 (2013).
[15] J. Zhao, Y. Li, G. Yang, K. Jiang, H. Linx, H. Ade, W. Ma, and H. Yan, Nature Energy **1**, 15027 (2016).
[16] R. J. M. Vullers, R. van Schaijk, I. Doms, C. Van Hoof, and R. Mertens, Solid-State Electron. **53**, 684 (2009).
[17] A. Hande, T. Polk, W. Walker, and D. Bhatia, Microprocess. Microsyst. **31**, 420 (2007).
[18] J. F. Randall and J. Jacot, Renew. Energy **28**, 1851 (2003).
[19] S. Mori, T. Gotanda, Y. Nakano, M. Saito, K. Todori, and M. Hosoya, Jpn. J. Appl. Phys. **54**, 071602 (2015).
[20] H. K. H. Lee, Z. Li, J. R. Durrant, and W. C. Tsoi, Appl. Phys. Lett. **108**, 253301 (2016).
[21] K. Tada, Polym. Bull. **73**, 2401 (2016).
[22] K. Tada, Org. Electron. **30**, 289 (2016).
[23] K. Tada, Phys. Status Solidi A **212**, 1731 (2015).
[24] I. Horcas, R. Fernandez, J.M. Gomez-Rodriguez, J. Colchero, J. Gomez-Herrero, and A. M. Baro, Rev. Sci. Instrum. **78**, 013705 (2007).
[25] http://www.wsxmsolutions.com/
[26] A. Rose, RCA Rev. **12**, 362 (1951).
[27] L. J. A. Koster, V. D. Mihailetchi, R. Ramaker, and P. W. M. Blom, Appl. Phys. Lett. **86**, 123509 (2005).
[28] G. J. Hedley, A. J. Ward, A. Alekseev, C. T. Howells, E. R. Martins, L. A. Serrano, G. Cooke, A. Ruseckas, and I. D. W. Samuel, Nature Commun. **4**, 2867 (2013).
[29] F. Liu, W.Zhao, J. R. Tumbleston, C. Wang, Y. Gu, D.Wang, A. L. Briseno, H. Ade, and T. P. Russell, Adv. Energy Mater. **4**, 1301377 (2014).
[30] P. E. Shaw, A. Ruseckas, and I. D. W. Samuel Adv. Mater. **20**, 3516 (2008).
[31] Z. He, B. Xiao, F. Liu, H. Wu, Y. Yang, S. Xiao, C. Wang,T. P. Russell, and Y. Cao, Nature Photon. **9**, 174 (2015).
[32] H. Yoshida, J. Phys. Chem. C **118**, 24377 (2014).
[33] C. Waldauf, P. Schilinsky, J. Hauch, and C. J. Brabec, Thin Solid Films **451–452**, 503 (2004).

